

Energy approach for dynamic buckling of shallow fixed arches under step loading with infinite duration

*Yong-Lin Pi¹, Mark Andrew Bradford¹ and Weilian Qu²

¹*School of Civil and Environmental Engineering, Faculty of Engineering and Information Technology, University of Technology, Sydney, Broadway, NSW 2007, Australia*

²*Key Laboratory of Roadway Bridge and Structural Engineering, Wuhan University of Technology, Wuhan 430070, China*

(Received February 2, 2009, Accepted February 23, 2010)

Abstract. Shallow fixed arches have a nonlinear primary equilibrium path with limit points and an unstable postbuckling equilibrium path, and they may also have bifurcation points at which equilibrium bifurcates from the nonlinear primary path to an unstable secondary equilibrium path. When a shallow fixed arch is subjected to a central step load, the load imparts kinetic energy to the arch and causes the arch to oscillate. When the load is sufficiently large, the oscillation of the arch may reach its unstable equilibrium path and the arch experiences an escaping-motion type of dynamic buckling. Nonlinear dynamic buckling of a two degree-of-freedom arch model is used to establish energy criteria for dynamic buckling of the conservative systems that have unstable primary and/or secondary equilibrium paths and then the energy criteria are applied to the dynamic buckling analysis of shallow fixed arches. The energy approach allows the dynamic buckling load to be determined without needing to solve the equations of motion.

Keywords: dynamic buckling; energy conservation; escaping-motion; lower dynamic buckling load; nonlinear equilibrium path; step loading of infinite duration; upper dynamic buckling load.

1. Introduction

Shallow fixed arches have a nonlinear primary equilibrium path with limit points and an unstable postbuckling equilibrium path, and they may also have bifurcation points at which equilibrium bifurcates from the nonlinear primary path to an unstable secondary equilibrium path. When an in-plane step load is applied to a shallow circular arch that is fully braced laterally (Fig. 1), the load will impart kinetic energy to the arch and cause the arch to oscillate about a stable equilibrium position. If this load is sufficiently large, the oscillation may reach an unstable equilibrium position, which may then induce dynamic buckling of the arch. The stability criterion of Laplace or Lagrange is used in this paper. According to this criterion, dynamic buckling is defined as a state at which an escaping motion either becomes unbounded or has very large amplitudes. The minimum load corresponding to this state is defined as the dynamic buckling load.

*Corresponding author, Professor, E-mail: YongLin.Pi@uts.edu.au

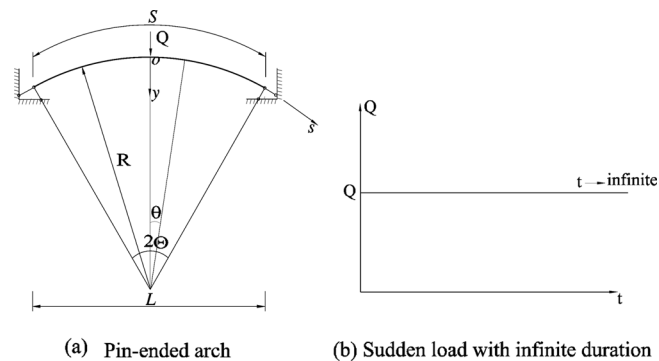


Fig. 1 A shallow fixed arch subjected to a sudden central load of infinite duration

The dynamic buckling of a structure under a general dynamic load is often solved using the equation of motion method. Numerical solutions of the equations of motion for various values of the load parameter to obtain the response of a structural system are often used for dynamic buckling analysis (Budiansky and Hutchinson 1964, Donaldson and Plaut 1983, Matsunaga 1996, Huang *et al.* 2003). The load parameter at which there exists a large change in the response is considered as the critical one. However, when the equation of motion approach is used to deal with the dynamic buckling of a continuum, the continuum needs to be reduced to a multi-degree-of-freedom system and the calculations require a large amount of time, which often makes its application very difficult for analysis. In addition, the accuracy of this approach often depends on the number of degrees-of-freedom of the reduced system and on the accuracy of the numerical method adopted (Matsunaga 1996, 2008, Huang *et al.* 2003). When this approach is applied to nonlinear systems, the difficulty is the intractability of the highly nonlinear differential equations of motion, despite of the availability of modern efficient computational techniques and high speed computers. The solutions of such nonlinear initial-value problems are quite sensitive to the initial conditions, and so the numerical difficulties may lead to less reliable and possibly erroneous solutions.

When a structure such as shallow arches and shells is subjected to a step load, the oscillation of the structure may reach the unstable equilibrium path and the structure experiences an escaping-motion type of buckling. Energy approaches can be used to derive for the dynamic buckling analysis of such structures. Simitse (1990) used energy approaches to study the dynamic buckling of suddenly loaded structures. Levitas *et al.* (1997) adopted Poincaré-like simple cell mapping to present a study of the global dynamic stability of a shallow elastic arch that is subjected to uniform constant radial loading. Pinto and Gonçalves (2000) investigated a strategy for the active non-linear control of the oscillation of a shallow arch-like simply supported buckled beam in order to prevent dynamic instability. Kounadis *et al.* (1999, 2004) developed energy and geometric methods, performed a number of investigations of the nonlinear dynamic buckling of autonomous systems, and proposed useful dynamic buckling criteria based on a geometric consideration. They studied the nonlinear dynamic buckling of autonomous non-dissipative N-degree-of-freedom systems (Kounadis *et al.* 2004), established dynamic instability criteria using characteristic distances associated with the geometry of the zero level total potential energy, and demonstrated the reliability and efficiency of the criteria by a comparison with the results based on the Verner-Runge-Kutta scheme. Kounadis and Raftoyiannis (2005) discussed non-linear dynamic buckling of a two degree-of freedom (2-DOF) imperfect planar system with symmetric imperfections under a step load of infinite duration

using energy and geometric considerations. Raftoyiannis *et al.* (2006) used Catastrophe Theory to investigate dynamic buckling of a simple geometrically imperfect frame. Sophianopoulos *et al.* (2008) adopted the Lienard-Chipart stability criterion to study the local instability of two degree of freedom weakly damped systems. Investigations of the dynamic buckling of shallow arches have hitherto concentrated on sinusoidal arches under loads distributed as half sine-waves (Lo and Masur 1976, Gregory and Plaut 1982, Simites 1990) using sine series methods. Matsunaga (1996) and Huang *et al.* (2003) used the method of power series expansion of the displacement components to investigate the free vibration and dynamic stability of circular arches, and presented an approximate theory for the dynamic buckling loads of shallow circular arches. In these studies, the coupling between the normal and axial deformations was not considered. Ignoring this coupling may be valid for very shallow sinusoidal arches. However, the coupling between the radial (normal) and axial displacements in a circular shallow arch is significant and so should be considered, particularly when exact closed form solutions are sought, as was pointed out by Bradford *et al.* (2002) and Pi *et al.* (2008). Pi and Bradford (2008) applied the energy approach to the dynamic buckling of pin-ended arches, considered the coupling of the radial and axial deformations, and obtained closed form solutions for the lower and upper dynamic buckling of the pin-ended arches.

This paper uses a 2-DOF arch model to derive the energy criteria for dynamic buckling of the conservative systems that have unstable primary and/or secondary equilibrium paths and applies the criteria to the in-plane dynamic buckling analysis of undamped shallow fixed circular arches that are subjected to a central step load of infinite duration.

2. Energy criteria for dynamic buckling

2.1 Static equilibrium and buckling of the two-degree-of-freedom system

The 2-DOF arch system proposed by Simites (1990) (Fig. 2) is used to establish the energy criteria for dynamic buckling. The system has three rigid massless bars AB , BC and CD pinned together by joints B and C . The rotations of B and C are restrained by linear rotational springs at B and C . The inclined angles θ_0 of AB and CD are initially equal to each other. The ends A and D of the two inclined bars AB and CD are simply supported. A horizontal linear spring is connected to the roller support D to restrain the horizontal motion of the end D . Two equal masses m are attached to the pin-joints B and C respectively. Two equal vertical step loads Q are applied to joints B and C of the system simultaneously. The motion of the system can be described by the angular displacement responses θ_1 and θ_2 of two rigid bars AB and CD , and the angular velocities $\dot{\theta}_1$ and $\dot{\theta}_2$ of two masses where $\dot{\theta} = \partial\theta/\partial t$ and t is the time.

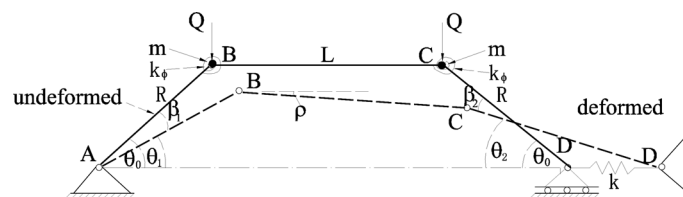


Fig. 2 A two degree-of-freedom arch model and loading

The total energy of the system can be expressed as

$$E = T + U \quad (1)$$

where the total potential energy U is given by

$$U = \frac{1}{2}\alpha[(\theta_0 - \gamma - \eta - \rho)^2 + (\theta_0 - \gamma + \eta + \rho)^2] + \frac{1}{2}(2\lambda\cos\eta\cos\gamma + \cos\rho - 2\lambda\cos\theta_0 - 1)^2 - 2Q^*\lambda(\sin\theta_0 - \cos\eta\cos\gamma) \quad (2)$$

and the kinetic energy T is given by

$$T = \frac{1}{2}\lambda^2(\dot{\gamma}^2 + \dot{\eta}^2) \quad (3)$$

in which the variables γ and η are defined by

$$\gamma = \frac{\theta_1 + \theta_2}{2} \quad \text{and} \quad \eta = \frac{\theta_1 - \theta_2}{2} \quad (4)$$

the dimensionless stiffness parameter of the springs α , the dimensionless load Q^* , and the ratio of bar lengths λ are defined by

$$\alpha = \frac{k_\phi}{kL^2}, \quad Q^* = \frac{Q}{kL}, \quad \lambda = \frac{R}{L} \quad (5)$$

and the angle ρ is given by

$$\rho = \arcsin[\lambda(\sin\theta_1 - \sin\theta_2)] \quad (6)$$

where k is the stiffness of the horizontal linear elastic spring, k_ϕ is the stiffness of the rotational springs, L is the length of the horizontal bar, and R is the length of the inclined bars. and $\dot{\gamma} = \partial\gamma/\partial\tau$ and $\dot{\eta} = \partial\eta/\partial\tau$ are the dimensionless angular velocity of the system, and the dimensionless time parameter τ is defined by $\tau = t\sqrt{k/m}$.

For static equilibrium, it is necessary that the derivatives of the total potential energy given by Eq. (2) with respect to the variables γ and η vanish, i.e.

$$\frac{\partial U}{\partial \gamma} = 0 \quad \text{and} \quad \frac{\partial U}{\partial \eta} = 0 \quad (7)$$

which leads to

$$\alpha\left[(\theta_0 - \gamma) + (\eta + \rho)\frac{2\lambda\sin\eta\sin\gamma}{\cos\rho}\right] + \lambda\sin\gamma(2\lambda\cos\eta\cos\lambda + \cos\rho - 2\lambda\cos\theta_0 - 1)(\cos\eta - \tan\rho\sin\eta) - Q^*\lambda\cos\eta\cos\gamma = 0 \quad (8)$$

and

$$\alpha(\eta + \rho)\left[1 + \frac{2\lambda\cos\eta\cos\lambda}{\cos\rho}\right] - \lambda\cos\gamma(2\lambda\cos\eta\cos\lambda + \cos\rho - 2\lambda\cos\theta_0 - 1)(\sin\eta + \tan\rho\cos\eta) - Q^*\lambda\sin\eta\sin\gamma = 0 \quad (9)$$

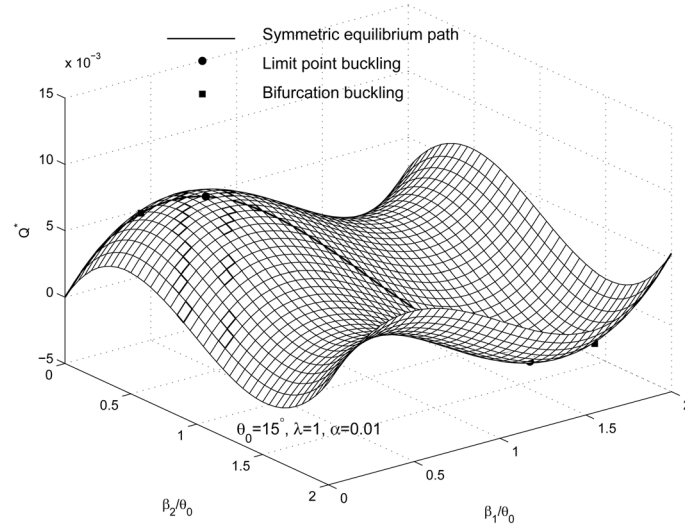


Fig. 3 Static equilibrium path

The surface described by Eqs. (8) and (9) for a system with the initial angle $\theta_0 = 15^\circ$, the ratio $\lambda = 1$, and the dimensionless stiffness parameter $\alpha = 0.01$ is shown in Fig. 3 as variations of the dimensionless load Q^* with the dimensionless angular displacements β_1/θ_0 and β_2/θ_0 where $\beta_1 = (\theta_0 - \theta_1)$ and $\beta_2 = (\theta_0 - \theta_2)$. The path of the symmetric deformations lies in the vertical plane formed by the Q^* axis and the line $\beta_1 = \beta_2$ (i.e., $\eta = 0$) as shown in Fig. 3. It can be seen from Fig. 3 that there exist limit points in the symmetric equilibrium path. The limit points of the symmetric curve can be determined by

$$\frac{\partial Q^*}{\partial \gamma} = 0 \Rightarrow \frac{\partial^2 U}{\partial \gamma^2} = 0 \quad (10)$$

which leads to

$$\alpha + 2\lambda^2(\sin^2 \gamma + \cos \theta_0 \cos \gamma - \cos^2 \gamma) - Q^* \lambda \sin \gamma = 0 \quad (11)$$

The arch system may also buckle in a bifurcation mode from a prebuckling symmetric equilibrium configuration defined by $\{\gamma, \eta, Q^*\}$ to a buckled equilibrium configuration defined by $\{\gamma + \gamma_b, \eta + \eta_b, Q^*\}$ under a constant load Q^* where γ_b and η_b are the infinitesimal buckling displacements. By considering the equilibrium at the configurations $\{\gamma, \eta, Q^*\}$ and $\{\gamma + \gamma_b, \eta + \eta_b, Q^*\}$, the condition for more than one equilibrium configuration in the close vicinity can be obtained as

$$[\alpha + 2\lambda^2(\sin^2 \gamma + \cos \theta_0 \cos \gamma - \cos^2 \gamma) - Q^* \lambda \sin \gamma] \gamma_b = 0 \quad (12)$$

and

$$[\alpha(1 + 2\lambda)^2 + 2\lambda^2(\cos \theta_0 \cos \gamma - \cos^2 \gamma) + 4\lambda^3(\cos \theta_0 - \cos \gamma) - Q^* \lambda \sin \gamma] \eta_b = 0 \quad (13)$$

For symmetric buckling, $\gamma_b \neq 0$, while for asymmetric buckling, $\eta_b \neq 0$. Hence, Eq. (12) leads to the condition for symmetric buckling given by Eq. (11) while Eq. (13) leads to the condition for asymmetric buckling as

$$\alpha(1 + 2\lambda)^2 + 2\lambda^2(\cos \theta_0 \cos \gamma - \cos^2 \gamma) + 4\lambda^3(\cos \theta_0 - \cos \gamma) - Q^* \lambda \sin \gamma = 0 \quad (14)$$

The buckling loads are also shown in Fig. 3. It can be seen that the magnitudes of the bifurcation buckling loads of this system are lower than those of the corresponding limit point buckling loads.

2.1 Equation of motion of a two-degree-of freedom system

The equations of motion for the 2-DOF arch system (Fig. 2) can be obtained as

$$\ddot{\theta}_1 + \alpha \left[\lambda(\theta_1 - \theta_2 + 2\rho) \frac{\cos \theta_1}{\cos \rho} + (\theta_1 - \theta_0 + \rho) \right] - \lambda[\lambda(\cos \theta_1 + \cos \theta_2) + \cos \rho - 2\lambda \cos \theta_0 - 1](\sin \theta_1 + \tan \rho \cos \theta_1) + Q^* \lambda \cos \theta_1 = 0 \quad (15)$$

and

$$\ddot{\theta}_2 + \alpha \left[\lambda(\theta_2 - \theta_1 - 2\rho) \frac{\cos \theta_2}{\cos \rho} + (\theta_2 - \theta_0 - \rho) \right] + \lambda[\lambda(\cos \theta_1 + \cos \theta_2) + \cos \rho - 2\lambda \cos \theta_0 - 1](\tan \rho \cos \theta_2 - \sin \theta_2) + Q^* \lambda \cos \theta_2 = 0 \quad (16)$$

The differential equations of motion given by Eqs. (15) and (16) can be solved simultaneously by numerical procedures such as the Runge-Kutta procedure. Dynamic buckling of a system with an initial inclined angle $\theta_1 = \theta_2 = \theta_0 = 20^\circ$, a dimensionless stiffness parameter $\alpha = 0.02$, and a ratio $\lambda = 1$ is investigated using Eqs. (15) and (16). It is assumed that at time $\tau = 0$, the system is at rest. Hence, the initial conditions are $\theta_1 = \theta_2 = \theta_0 = 20^\circ$ and $\dot{\theta}_1 = \dot{\theta}_2 = 0$. The results by the Runge-Kutta procedure are shown in Fig. 4 as variations of the dimensionless angular displacement responses β_1/θ_0 and β_2/θ_0 with the dimensionless time τ . It can be seen that when the step load $Q^* =$

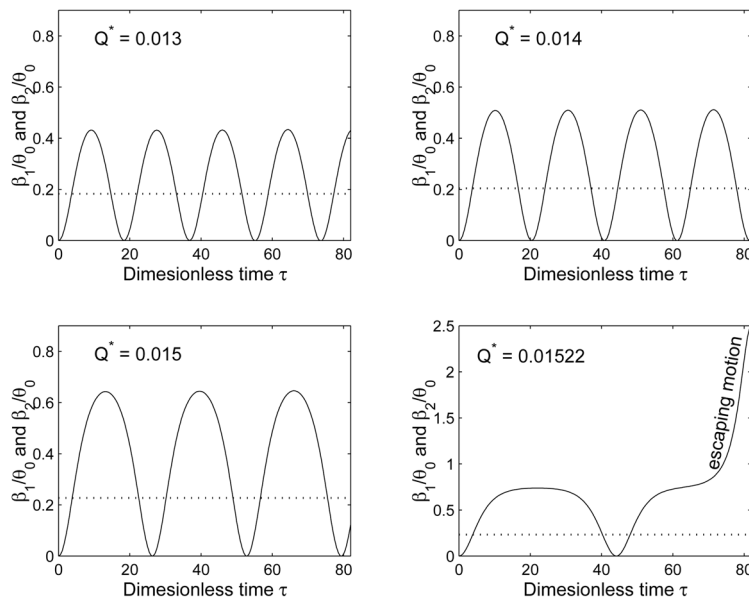


Fig. 4 Symmetric escaping motion of the 2-DOF system

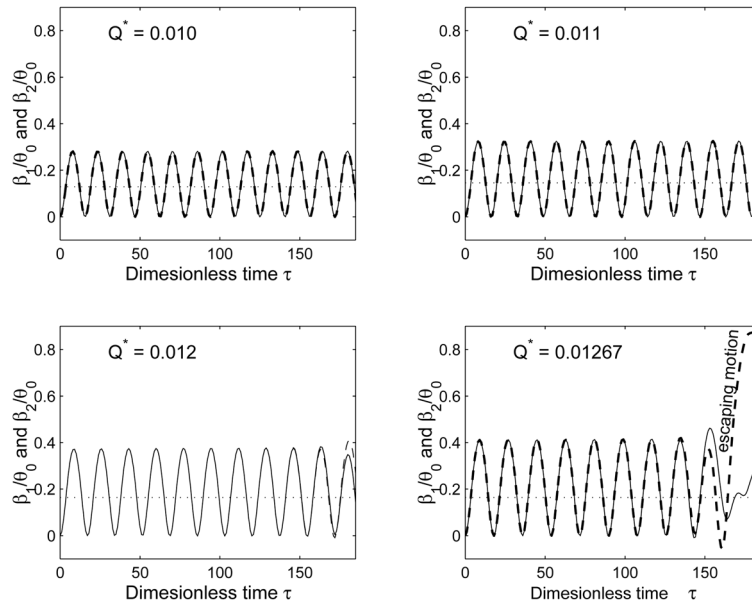


Fig. 5 Asymmetric escaping motion of the 2-DOF system

0.013, 0.014, or 0.015 is applied, the system simply oscillates about a stable equilibrium position. When the step load $Q^* = 0.01522$ is applied, the amplitude of the motion of the system becomes so large that an escaping motion, i.e., dynamic buckling of the system, occurs. Because the initial conditions are symmetric, only the symmetric responses were obtained and the angular displacement responses for β_1/θ_0 coincide with β_2/θ_0 as shown in Fig. 4.

In addition to symmetric dynamic buckling, asymmetric dynamic buckling of the system is possible. To produce asymmetric responses of the system, slightly different values are assigned to the initial angles as $\theta_1 = \theta_0 + 2^\circ \times 10^{-9}$, $\theta_2 = \theta_0$, and $\dot{\theta}_1 = \dot{\theta}_2 = 0$. The results are shown in Fig. 5 as variations of the dimensionless angular displacement responses β_1/θ_0 and β_2/θ_0 with the dimensionless time τ . It can be seen that when the step load $Q^* = 0.010$, 0.011 , or 0.012 is applied, the motion of the system is simply oscillatory. When the step load $Q^* = 0.01267$ is applied, the amplitude of the motion of the system becomes so large that escaping motion occurs. It can also be seen that for the small step load $Q^* = 0.010$ or 0.011 , the oscillation of the system is still symmetric in the range of integration ($\tau = 185$) although the initial condition is asymmetric. For the step loads $Q^* = 0.012$ and 0.01267 , the asymmetric oscillation occurs at $\tau = 180$ and 150 , respectively.

2.3 Energy criteria for dynamic buckling

Because the structure and step loads form a conservative system, the total energy of the system must satisfy the principle of energy conservation, i.e., the total energy of the system has to be equal to a constant during the motion of the system. The value of the constant is determined from the initial condition. Because the system is at rest initially, which means that there are no deformations (i.e., the angular responses θ_1 , θ_2 are equal to its initial angle θ_0) and the velocities are equal to zero $\dot{\theta}_1, \dot{\theta}_2$ at time $t = 0$. Hence, the total energy E at $t = 0$ is equal to zero. According to the

principle of energy conservation, for $t \geq 0$

$$\mathbf{E} = U + T = U + \frac{1}{2}\lambda^2(\dot{\gamma}^2 + \dot{\eta}^2) = 0 \quad (17)$$

It can be seen from Eqs. (3) and (17) that the kinetic energy T of the system is a positive definite function of the velocities $\dot{\gamma}$ and $\dot{\eta}$. Hence, to satisfy the principle of energy conservation given by Eq. (17), motion of the system is possible only when the total potential energy U is non-positive. In this case, the step loading imparts kinetic energy and deformation potential energy (or spring energy) to the system, and causes the system to oscillate about an equilibrium position. When the step loads are small, the total potential energy at a stable equilibrium position is negative and so the system oscillates about this position. The oscillation amplitudes increase with an increase of the loads. When the step loads become so large that the total potential energy at an unstable equilibrium position is non-positive, the oscillation of the system may reach an unstable equilibrium position and the system may buckle dynamically at the unstable equilibrium position. Hence, for a possible dynamic buckling of the system, $U \leq 0$, i.e., the critical condition is $U = 0$. This can also be justified by searching for stationary points of the total energy \mathbf{E} given by Eq. (1).

Because the dynamic buckling occurs when the oscillation of the system reaches one of unstable static equilibrium positions of the system, the oscillation reaches one of its extrema. From calculus, the necessary conditions for extrema of the total energy \mathbf{E} can be expressed as

$$\frac{\partial \mathbf{E}}{\partial \gamma} = 0, \quad \frac{\partial \mathbf{E}}{\partial \eta} = 0 \quad (18)$$

and

$$\frac{\partial \mathbf{E}}{\partial \dot{\gamma}} = 0, \quad \frac{\partial \mathbf{E}}{\partial \dot{\eta}} = 0 \quad (19)$$

Substituting Eq. (2) into Eqs. (18) and (19) leads to these necessary conditions as

$$\frac{\partial U}{\partial \gamma} = 0, \quad \frac{\partial U}{\partial \eta} = 0 \quad (20)$$

and

$$\frac{\partial U}{\partial \dot{\gamma}} = 0, \quad \frac{\partial U}{\partial \dot{\eta}} = 0 \quad (21)$$

Substituting Eq. (3) into Eq. (21) leads to

$$\dot{\gamma} = \dot{\eta} = 0 \quad (22)$$

from which, during dynamic buckling, the kinetic energy of the system vanishes as

$$T = \frac{1}{2}\lambda^2(\dot{\gamma}^2 + \dot{\eta}^2) = 0 \quad (23)$$

Substituting this equation into Eq. (17) leads to another necessary condition for dynamic buckling of the system as

$$U = 0 \quad (24)$$

which indicates that during dynamic buckling, the potential energy of load is equal to the deformation energy (or spring energy) of the system.

Eqs. (20) and (24) form the necessary conditions for dynamic buckling of the system. The dynamic buckling load Q_D^* and the corresponding angular displacement responses γ_D and η_D can be obtained by solving Eqs. (20) and (24) simultaneously.

Applying the necessary conditions given by Eqs. (20) and (24) to the problem investigated in the section 2.2 leads to two solutions: $Q^* = 0.01267$ and $Q^* = 0.01522$ which are the same as those obtained by the method of equations of motion. The lower dynamic buckling load $Q^* = 0.01267$ corresponds to the saddle points of the total potential energy surface and the total potential energy at the saddle points vanishes as shown in Fig. 6. The upper dynamic buckling load $Q^* = 0.01522$ is

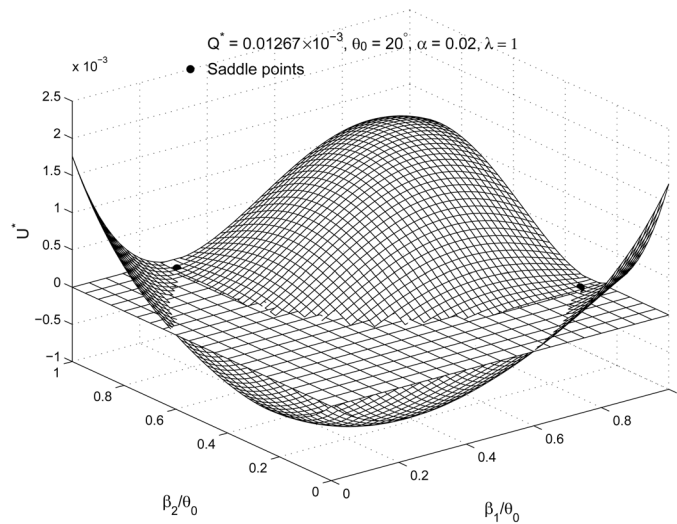


Fig. 6 Saddle points and lower dynamic buckling load

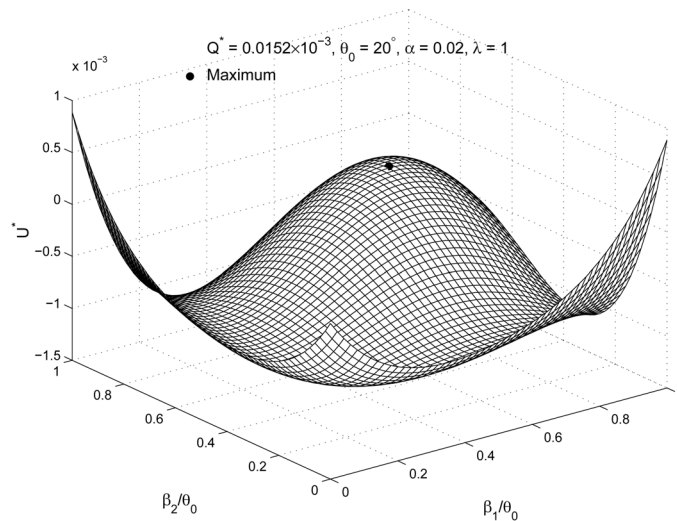


Fig. 7 Maximum point and upper dynamic buckling load

associated with the maximum of the total potential energy surface and the total potential energy at the maximum vanishes as shown in Fig. 7. The nature of the dynamic buckling loads obtained from the necessary conditions given by Eqs. (20) and (24) can be determined by the nature of the corresponding stationary points. The condition for the upper dynamic buckling load is that

$$\frac{\partial^2 U}{\partial \theta_1^2} < 0, \quad \frac{\partial^2 U}{\partial \theta_2^2} < 0 \quad (25)$$

and

$$\left(\frac{\partial^2 U}{\partial \theta_1 \partial \theta_2} \right)^2 < \frac{\partial^2 U}{\partial \theta_1^2} \times \frac{\partial^2 U}{\partial \theta_2^2} \quad (26)$$

The second order partial derivatives of the total potential energy for the upper buckling load $Q^* = 0.01522$ satisfy both conditions given by Eqs. (25) and (26).

The condition for the lower dynamic buckling load is that

$$\frac{\partial^2 U}{\partial \theta_1^2} \quad \text{and} \quad \frac{\partial^2 U}{\partial \theta_2^2} \quad (27)$$

have opposite signs, or that

$$\left(\frac{\partial^2 U}{\partial \theta_1 \partial \theta_2} \right)^2 > \frac{\partial^2 U}{\partial \theta_1^2} \times \frac{\partial^2 U}{\partial \theta_2^2} \quad (28)$$

The second order partial derivatives of the total potential energy for the lower buckling load $Q^* = 0.01267$ satisfy the conditions given by Eqs. (27) and (28).

The energy criteria for determination of dynamic buckling loads of an undamped conservative system under step loading of infinite duration can be summarized as

- (1) the static equilibrium path of the system has an unstable branch;
- (2) the dynamic buckling occurs at an unstable static equilibrium point;
- (3) the total potential energy of the system vanishes at the unstable static equilibrium point.

3. In-plane dynamic buckling of shallow fixed arches

3.1 In-plane static equilibrium of shallow fixed arches

The energy criteria developed in the previous section is applied to the dynamic buckling of an undamped shallow fixed arch that is subjected to a central step load. The total energy E of the arch and load system consists of kinetic and potential energies as

$$E = T + U \quad (29)$$

where T and U are the kinetic and potential energies and are given by

$$T = \frac{1}{2} \int_V m \dot{v}^2 dV = \frac{mA}{2} \int_{-\Theta}^{\Theta} R^3 \dot{v}^2 d\theta \quad \text{and} \quad U = \frac{1}{2} \int_{-\Theta}^{\Theta} \int_A R \sigma \epsilon dA d\theta - \int_{-\Theta}^{\Theta} \bar{\delta}(\theta) Q R \tilde{v} d\theta \quad (30)$$

in which m is the mass density per unit length of the arch, R is the radius of initial curvature of the arch, A is the area of the cross-section, $\dot{v} = d\tilde{v}/dt$ is the velocity in the radial direction and

$\tilde{v} = v/R$, v is the radial displacement of the centroid, $\bar{\delta}(\theta)$ is the Dirac-delta, σ and ε are the longitudinal normal stress and strain and they are given by

$$\sigma = E\varepsilon, \quad \varepsilon = \tilde{w}' - \tilde{v} + \tilde{v}'^2/2 - y\tilde{v}''/R \quad (31)$$

where E is the Young's modulus, $(\)' = \partial(\)/\partial\theta$, θ is the angular coordinate, $\tilde{w} = w/R$, w is the axial displacement of the centroid, and y is the coordinate in the principal axis system of the cross-section.

For static analysis, the kinetic energy vanishes and it has been shown by Bradford *et al.* (2002) and Pi *et al.* (2008) that the axial compressive force N in the arch is constant and that the differential equation of equilibrium in the radial direction can be expressed as

$$\frac{\tilde{v}^{iv}}{\mu^2} + \tilde{v}'' = \frac{\delta(\theta)Q}{N} - 1 \quad \text{with} \quad \mu = \frac{NR^2}{EI} \quad (32)$$

and the boundary conditions at fixed ends $\theta = \pm\Theta$ are $\tilde{v} = \tilde{v}' = 0$, where I is the second moment of area of the cross-section about its major principal axis.

The solution for the radial displacement can be obtained from Eq. (32) as (Bradford *et al.* 2002, Pi *et al.* 2008)

$$\begin{aligned} \tilde{v} = & \frac{\mu\Theta[\cos(\mu\Theta) - \cos(\mu\theta)]}{\mu^2 \sin(\mu\Theta)} + \frac{\Theta^2 - \theta^2}{2} \\ & + \frac{Q^*}{\mu^3 \Theta} \left\{ \tan\left(\frac{\mu\Theta}{2}\right) [\cos(\mu\theta) + 1] - \mu\Theta - H(\theta) [\sin(\mu\theta) - \mu\theta] \right\} \end{aligned} \quad (33)$$

where Q^* is the dimensionless central load and $H(\theta)$ is a step function and they are defined by

$$Q^* = \frac{QR^2\Theta}{2EI} \quad \text{and} \quad H(\theta) = 1 \quad \text{for} \quad \theta > 0 \quad \text{or} \quad -1 \quad \text{for} \quad \theta < 0 \quad (34)$$

It was shown (Bradford *et al.* 2002, Pi *et al.* 2008) that the axial compressive force has a nonlinear relationship with the central load, which can be expressed as

$$A_1(Q^*)^2 + B_1Q^* + C_1 = 0 \quad (35)$$

where

$$A_1 = \frac{\mu\Theta[2 + \cos(\mu\Theta)] - 3\sin(\mu\Theta)}{2\mu^5\Theta^5[1 + \cos(\mu\Theta)]}, \quad B_1 = \frac{\mu\Theta - \sin(\mu\Theta)}{2\mu^3\Theta^3[1 + \cos(\mu\Theta)]} \quad (36)$$

$$C_1 = \left(\frac{\mu\Theta}{\lambda}\right)^2 + \frac{\mu\Theta - \sin(\mu\Theta)\cos(\mu\Theta)}{4\mu\Theta\sin^2(\mu\Theta)} - \frac{1}{6} \quad \text{with} \quad \lambda = \frac{R\Theta^2}{r} \quad (37)$$

in which $r = \sqrt{I/A}$ is the radius of gyration of the cross-section about its major principal axis.

3.2 Static limit point buckling and bifurcation buckling

Eq. (35) can be rewritten as an implicit function $F(Q^*, \mu) = 0$ of the load Q^* and the axial force parameter μ . The equation for the static upper (and lower) limit point buckling load can then be obtained by setting

$$\partial Q^*/\partial \mu = -[\partial F(Q^*, \mu)/\partial \mu]/[\partial F(Q^*, \mu)/\partial Q^*] = 0 \quad (38)$$

which leads to

$$A_2(Q^*)^2 + B_2Q^* + C_2 = 0 \quad (39)$$

with

$$A_2 = \frac{5}{2}A_1 + \frac{\sin(\mu\Theta)[\sin(\mu\Theta) - \mu\Theta]}{4\mu^4\Theta^4[1 + \cos(\mu\Theta)]^2}, \quad B_2 = \frac{3B_1}{2} + \frac{2\mu\Theta[1 - \cos(\mu\Theta)] - 3\sin(\mu\Theta)}{8\mu^2\Theta^2\sin(\mu\Theta)[1 + \cos(\mu\Theta)]} \quad (40)$$

$$C_2 = \frac{\cos(\mu\Theta)[2\mu^2\Theta^2 - \sin^2(\mu\Theta)]}{8\mu\Theta\sin^3(\mu\Theta)} - \frac{1}{8\sin^2(\mu\Theta)} - \left(\frac{\mu\Theta}{\lambda}\right)^2 \quad (41)$$

Solving Eqs. (35) and (39) simultaneously leads to exact solutions for static limit point buckling loads and the corresponding axial compressive forces.

In addition to static limit point buckling, an arch may buckle in a bifurcation mode, which is associated with antisymmetric buckling displacements. It has been shown (Bradford *et al.* 2002, Pi *et al.* 2008) that for bifurcation antisymmetric buckling of shallow fixed arches, it is required that

$$\tan(\mu\Theta) = \mu\Theta \quad (42)$$

whose lowest solution is $\mu\Theta \approx 1.4303\pi$. Substituting this into Eq. (35) leads to the equation for bifurcation antisymmetric static buckling loads as

$$\frac{1.167}{\pi^5}Q^{*2} - \frac{1.194}{\pi^3}Q^* + \frac{0.823}{\pi^2} + \frac{20.19}{\lambda^2} = 0 \quad (43)$$

Typical static equilibrium path and buckling behaviour of shallow fixed arches are shown in Fig. 8 for a shallow fixed arch with a length $S = 21.6$ m, a geometric parameter $\lambda = 50$, and a radius of gyration of the cross-section $r = 0.108$ m. It can be seen that the limit point buckling dominates the static buckling behaviour of fixed arches and that the bifurcation buckling occurs at the unstable descending branch of the primary equilibrium path (Bradford *et al.* 2002). This is different from shallow pin-ended arches. For most of shallow pin-ended arches, the bifurcation buckling dominates its buckling behaviour and bifurcation buckling occurs at the stable ascending branch of the primary equilibrium path (Bradford *et al.* 2002, Pi *et al.* 2008).

3.3 In-plane dynamic buckling

Because the arch and step load form a conservative system, the total energy of the system must satisfy the principle of energy conservation, i.e., the total energy of the system has to be constant during the motion of the system. The value of the total energy can be determined from the initial condition. Because the system is at rest and unstressed initially, i.e., the strain $\varepsilon = 0$, the velocity $\dot{v} = 0$ and $Q = 0$ at time $t = 0$, from Eq. (29), the initial total energy $E = 0$ at time $t = 0$. From the principle of energy conservation, for time $t \geq 0$, the total energy of the system still vanishes, i.e.

$$E = T + U = 0 \quad \forall t \geq 0 \quad (44)$$

When the central step load is applied to the arch, it imparts kinetic energy and strain energy to the system, and causes the system to oscillate about an equilibrium position. From Eq. (30), the kinetic

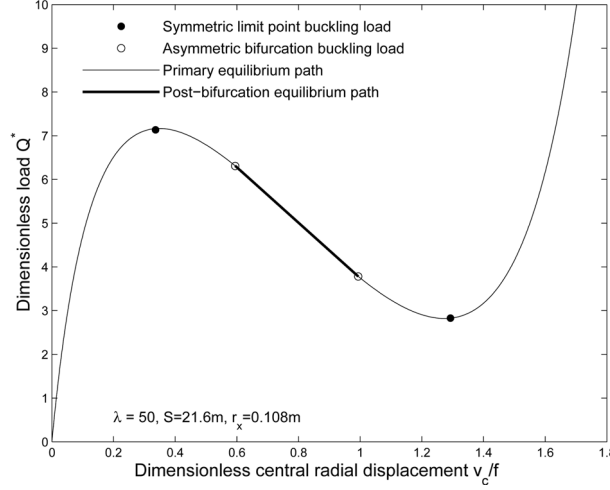


Fig. 8 Static equilibrium and buckling of shallow fixed arches

energy T of the system is a positive definite function of the velocity \dot{v} . Hence, from Eq. (44), motion of the system is possible when the total potential energy U is non-positive.

From the static analysis, for a load that is higher than a certain value, it corresponds to a near stable equilibrium position, an unstable equilibrium position, or a remote stable equilibrium position (Fig. 8). When the step load is small, the total potential energy of the system at the corresponding near stable equilibrium position is negative and so the system oscillates about this position. However, under the small load, the total potential energy of the arch system at the corresponding unstable equilibrium position is positive and the total energy of the arch does not vanish. Hence, the principle of energy conservation is not satisfied and the motion of the arch system to the unstable equilibrium position is impossible. As the value of the step load increases, the total potential energy of the system at the unstable equilibrium position decreases and the oscillation amplitudes of the system increase. When the step load is so large that the total potential energy of the system at the corresponding unstable equilibrium position becomes zero and from the principle of energy conservation, the oscillation of the system reaches the unstable equilibrium position and dynamic buckling of the arch system occurs. Hence, vanishing of the total potential energy U of the arch system is a necessary condition for the dynamic buckling of a shallow fixed arch under a step load of infinite duration. By substituting Eqs. (31) and (33), vanishing of the total potential energy of the shallow fixed arch given by Eq. (30) can be expressed as

$$U = A_3(Q^*)^2 + B_3Q^* + C_3 = 0 \quad (45)$$

where

$$A_3 = \frac{\mu\Theta[1 + 4\cos^2(\mu\Theta/2)] - 5\sin(\mu\Theta)}{2\mu^2\Theta^2\cos^2(\mu\Theta/2)}, \quad B_3 = \frac{3\sin(\mu\Theta) - \mu\Theta[1 + 2\cos^2(\mu\Theta/2)]}{2\cos^2(\mu\Theta/2)} \quad (46)$$

$$C_3 = \frac{\mu^5\Theta^5}{\lambda^2} + \frac{\mu^2\Theta^2\cot(\mu\Theta)}{2} + \frac{\mu^3\Theta^3}{2\sin^2(\mu\Theta)} - 1 \quad (47)$$

Because the dynamic buckling occurs at an unstable equilibrium position, the dynamic buckling load also needs to satisfy the equilibrium equation given by Eq. (35). The dynamic buckling load and the corresponding axial forces can then be obtained by solving Eqs. (35) and (45) simultaneously and the corresponding unstable equilibrium position can be determined using Eq. (33). The equilibrium equation given by Eq. (35) describes the primary symmetric deformation of the arch and the load obtained is the upper dynamic buckling load.

The total potential energy U may also vanish on the secondary bifurcation unstable equilibrium path. It has been shown that at the secondary bifurcation unstable equilibrium path of a shallow fixed arch, $\mu\Theta \approx 1.4303\pi$ (Pi and Bradford 2009). Substituting this into Eq. (45) leads to the necessary condition for the lower dynamic buckling load as

$$1.038Q^{*2} - 13.975Q^* + 45.363 + \frac{(1.4303\pi)^5}{\lambda^2} = 0 \tag{48}$$

Typical solutions for the upper and lower dynamic buckling loads for a shallow fixed arch with a length $S = 21.6$ m, a geometric parameter $\lambda = 60$, and a radius of gyration of the cross-section $r = 0.108$ m are shown in Fig. 9, where the solid line is the primary equilibrium path under static loading, the dashed line is the secondary equilibrium path after bifurcation buckling, and the dot-dashed line represents the zero total potential energy ($U = 0$). The intersection point d_u of the curve of zero total potential energy and the primary unstable equilibrium path $a_s b_s$ defines the upper dynamic buckling load while the intersection point d_l of the curve of zero total potential energy and the secondary equilibrium path ab defines the lower dynamic buckling load. Variations of the dimensionless upper and lower dynamic buckling loads Q^* with the geometric parameter λ are shown in Fig. 10 for fixed arches with a length $S = 21.6$ m and a radius of gyration of the cross-section $r = 0.108$ m. It can be seen that the dynamic buckling load Q^* increases with an increase of the geometric parameter λ . For comparison, variations of the static limit point buckling loads and the bifurcation buckling load with the geometric parameter λ are also shown in Fig. 10 for these fixed arches. It can be seen that both the upper and lower dynamic buckling loads are lower than the corresponding static buckling loads. It can also be seen that when the geometric parameter $\lambda =$

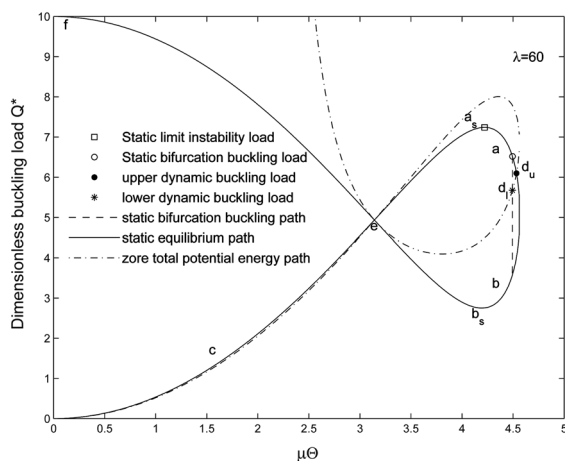


Fig 9 Upper and lower dynamic buckling loads

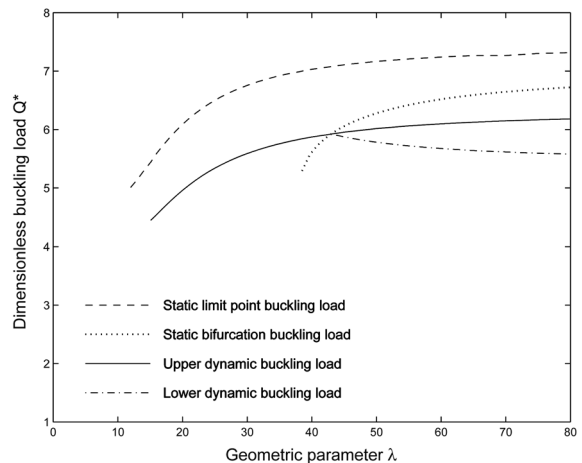


Fig. 10 Comparisons of dynamic buckling loads with their static counterpart for fixed arches

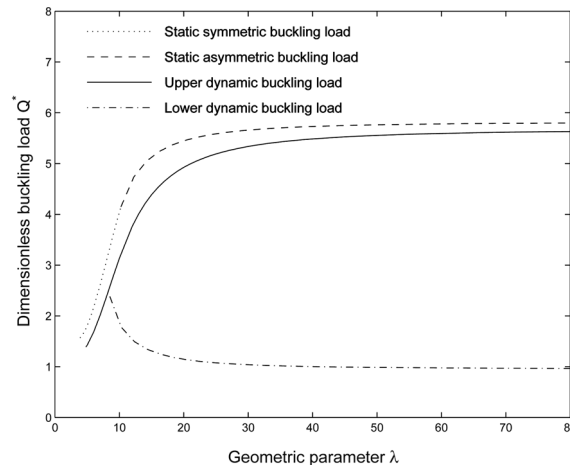


Fig. 11 Comparisons of dynamic buckling loads with their static counterpart for pin-ended arches

43, the upper and lower dynamic buckling loads are equal to each other and $Q^* = 5.925$, which can be obtained by substituting $\mu\Theta \approx 1.4303\pi$ into Eqs. (35) and (45) and solving them for the dynamic load Q^* and λ . For shallow fixed arches with the geometric parameter $\lambda < 43$, there is no lower dynamic buckling.

The results for the dynamic and static buckling loads for pin-ended arches with the same length S and radius gyration r (Pi and Bradford 2008) are shown in Fig. 11 for comparison. It can be seen that both the upper and lower dynamic buckling loads are lower than the corresponding static buckling loads. It can also be seen that the lower dynamic buckling loads of pin-ended arches are much lower than their upper counterparts. However, the lower dynamic buckling loads of fixed arches are only slightly lower than their upper counterparts (Fig. 10). When the geometric parameter $\lambda = 8.25$, the lower and upper dynamic buckling loads are equal to each other and $Q^* = 2.477$. For shallow pin-ended arches with the geometric parameter $\lambda < 8.25$, there is no lower buckling load.

4. Conclusions

A 2-DOF arch model was used to develop energy criteria for the dynamic buckling of a conservative undamped system under step loading of infinite duration based on the principle of conservation of energy. Comparison with the results of equation of motion method showed the results obtained from the energy method are accurate. The energy criteria were applied to the dynamic buckling analysis of shallow fixed circular arches under a central step load of infinite duration. The exact primary equilibrium path and the secondary equilibrium path after bifurcation were obtained, which are essential for the dynamic buckling analysis using energy approaches. Analytical solutions for the upper and lower dynamic buckling loads of shallow fixed arches under a central step loading with infinite duration were derived. It was found that the upper and lower dynamic buckling loads of a shallow fixed arch due to the central step loading is lower than its static limit point buckling and bifurcation buckling loads. The energy approach allows the dynamic buckling load to be determined without the need to solve the equations of motion of the arch system.

Acknowledgements

This work has been supported by the Australian Research Council through Discovery Projects and a Federation Fellowship awarded to the second author. The third author has been supported by Chinese National Natural Science Foundation through a Key Program (No. 50830203).

References

- Bradford, M.A., Uy, B. and Pi, Y.L. (2002), "In-plane stability of arches under a central concentrated load", *J. Eng. Mech.-ASCE*, **128**(7), 710-719.
- Budiansky, B. and Hutchinson, J.W. (1964), "Dynamic buckling of imperfection-sensitive structures", *Proceedings of XI International Congress of Applied Mechanics*, Munich.
- Donaldson, M.T. and Plaut, R.H. (1983), "Dynamic stability boundaries of a sinusoidal shallow arch under pulse loads", *AIAA J.*, **21**(3), 469-471.
- Gregory, W.E. Jr and Plaut, R.H. (1982), "Dynamic stability boundaries for shallow arches", *J. Eng. Mech. Div.-ASCE*, **108**(6), 1036-1050.
- Huang, C.S., Nieh, K.Y. and Yang, M.C. (2003), "In-plane free vibration and stability of loaded and shear deformable circular arches", *Int. J. Solids Struct.*, **40**(22), 5865-5886.
- Kounadis, A.N., Gantes, C.J. and Bolotin, V.V. (1999), "Dynamic buckling loads of autonomous potential system based on the geometry of the energy surface", *Int. J. Eng. Sci.*, **37**(12), 1611-1628.
- Kounadis, A.N., Gantes, C.J. and Raftoyiannis, I.G. (2004), "A geometric approach for establishing dynamic buckling load of autonomous potential N-degree-of-freedom systems", *Int. J. Nonlin. Mech.*, **39**(12), 1635-1646.
- Kounadis, A.N. and Raftoyiannis, I.G. (2005), "Dynamic buckling of a 2-DOF imperfect system with symmetric imperfections", *Int. J. Nonlin. Mech.*, **40**(10), 1229-1237.
- Levitas, J., Singer, J. and Weller, T. (1997), "Global dynamic stability of a shallow arch by Poincaré-like simple cell mapping", *Int. J. Nonlin. Mech.*, **32**(2), 411-424.
- Lo, D.L.C. and Masur, E.F. (1976), "Dynamic buckling of shallow arches", *J. Eng. Mech. Div.-ASCE*, **102**(3), 901-917.
- Matsunaga, H. (1996), "In-plane vibration and stability of shallow circular arches subjected to axial forces", *Int. J. Solids Struct.*, **33**(4), 469-482.
- Matsunaga, H. (2008), "Free vibration and stability of functionally graded shallow shells according to a 2D higher-order deformation theory", *Compos. Struct.*, **84**(2), 132-146.
- Pi, Y.L., Bradford, M.A. and Tin-Loi, F. (2008), "Nonlinear in-plane buckling of rotationally restrained shallow arches under a central concentrated load", *Int. J. Nonlin. Mech.*, **43**(1), 1-17.
- Pi, Y.L. and Bradford, M.A. (2008), "Dynamic buckling of shallow pin-ended arches under a sudden central concentrated load", *J. Sound Vib.*, **317**(3-5), 898-917.
- Pi, Y.L. and Bradford, M.A. (2009), "Non-linear in-plane postbuckling of arches with rotational end restraints under uniform radial loading", *Int. J. Nonlin. Mech.*, **44**(9), 975-989.
- Pinto, O.C. and Gonçalves, P.B. (2000), "Non-linear control of buckled beams under step loading", *Mech. Syst. Signal Pr.*, **14**(6), 967-985.
- Raftoyiannis, I.G., Constantakopoulos, T.G., Michaltsos, G.T. and Kounadis, A.N. (2006), "Dynamic buckling of a simple geometrically imperfect frame using Catastrophe Theory", *Int. J. Mech. Sci.*, **48**(10), 1021-1030.
- Simitses, G.J. (1990), *Dynamic Stability of Suddenly Loaded Structures*, Springer-Verlag, New York, N.J.
- Sophianopoulos, D.S., Michaltsos, G.T. and Kounadis, A.N. (2008), "The effect of infinitesimal damping on the dynamic instability mechanism of conservative systems", *Math. Probl. Eng.*, Article ID 471080.